

Fabrication of a Graded-Index Circular-Core Polymer Parallel Optical Waveguide Using a Microdispenser for a High-Density Optical Printed Circuit Board

Kazutomo Soma and Takaaki Ishigure, *Member, IEEE*

Abstract—A simple fabrication method for multimode polymer optical waveguides with graded-index (GI) circular cores is introduced for use in optical printed circuit boards (O-PCBs). The new method, named “Mosquito method,” utilizes a microdispenser to dispense a viscous monomer directly onto the substrates. By optimizing the dispensing conditions, 12-channel parallel waveguides with circular GI-cores (core diameter of 40 μm) are successfully fabricated using the Mosquito method. The advantages of GI-core waveguides for O-PCB applications are discussed by comparing the optical characteristics of the fabricated waveguides with those of conventional step-index (SI) square-core polymer waveguides, and even with those of silica-based GI multimode fibers (MMFs), as an ideal case. To the best of our knowledge, this is the first comparison of SI- and GI-core multimode polymer waveguides that are composed of the same polymer materials and that have similar core and pitch sizes. We experimentally demonstrate that the GI circular-core polymer waveguides fabricated by the Mosquito method have sufficiently low propagation loss (0.033 dB/cm at 850 nm), low connection loss with GI-MMFs, and low interchannel crosstalk. We observe approximately -50 dB of interchannel crosstalk in the 250- μm pitch GI-core waveguide fabricated, which is almost 10 dB lower than in the SI counterpart. Furthermore, sufficiently low crosstalk is maintained in a half-pitch GI-core waveguide fabricated by the Mosquito method.

Index Terms—Graded-index (GI) core, on-board interconnection, optical printed circuit board (O-PCB), polymer optical waveguide.

I. INTRODUCTION

CURRENTLY, electrical wirings play the main role on printed circuit boards (PCBs) even in high-performance computers (HPCs), high-end routers, and servers. However, with increasing the processing speed of the chips on the boards, optical interconnection technologies have been drawing much attention, and in particular, multimode optical fiber (MMF) links are gradually deployed in rack-to-rack interconnects in HPC systems [1]. In the coming decades, to maintain the advancement of computing performance, not only the processing speed but also the power dissipation of the system is of great concern [2].

Thus, optical interconnect technologies have been regarded as a promising solution to address these problems, and optical PCB (O-PCB) technologies are expected to decrease the distance of electrical wiring on PCBs [3], [4].

Because of the compatibility with PCBs, multimode polymeric optical waveguides have been a promising component, and thus wide varieties of reports on polymer waveguides are available [5]–[8]. In particular, with the development of MMF links for short-reach networks, optical modules based on vertical cavity surface emitting lasers (VCSELs) have become a commodity, and thus O-PCBs with polymer waveguides are expected to have much promise. However, typical polymer optical waveguides have had square-shaped cores with a uniform refractive index, namely step-index (SI) type. Since, almost all of these polymer waveguides were expected to be utilized only in a point-to-point link in which a light source and detector are connected with a several-centimeter-long polymer waveguide, a propagation loss of 0.1 dB/cm or higher and large modal dispersion of the SI-core polymer waveguides were acceptable. However, over the last couple of years, since data rates of 20 Gbps and higher with a link distance of 0.5 to 1 m have been expected to be covered by polymer waveguides on PCBs, it is necessary to optimize the link power budget for an O-PCB.

For minimizing the power budget of polymer waveguide-based links, we proposed to introduce graded-index (GI) cores even into planar polymer waveguides for O-PCBs [9], and we have experimentally and theoretically demonstrated the capability of high-density and high-speed parallel optical links with GI-core polymer optical waveguides [10]–[13]. However, since we previously fabricated the GI-core waveguides using the preform method, in which a preform plate was heat drawn to a waveguide at 230 $^{\circ}\text{C}$, the thermal stability of the waveguides was of great concern.

It was difficult to utilize a cross-linkable, high-heat-resistance polymer to the preform method. Furthermore, as the waveguides are independently fabricated from PCBs, the process of integrating the waveguides on PCBs was another concern.

Therefore, in order to address the problems in the previously fabricated GI-core polymer waveguides, in this paper we focus on a new fabrication method for GI-core waveguides using a microdispenser. This method makes it possible to fabricate waveguides directly on-board using high-heat resistance polymers. Trials to fabricate polymer waveguides using a dispenser or utilizing the ink-jet printing technique are already reported, but as far as we know, it seems difficult to continuously form circular- or even square-shaped cores in those trials [14], [15].

Manuscript received May 31, 2012; revised August 5, 2012 and October 9, 2012; accepted October 26, 2012. Date of publication November 16, 2012; date of current version April 3, 2013.

K. Soma is with the Graduate School of Science and Technology, Keio University, Yokohama 223-8522, Japan (e-mail: kazu-so-much@a5.keio.jp).

T. Ishigure is with the Faculty of Science and Technology, Keio University, Yokohama 223-8522, Japan (e-mail: ishigure@appi.keio.ac.jp).

Color versions of one or more of the figures in this paper are available online at <http://ieeexplore.ieee.org>.

Digital Object Identifier 10.1109/JSTQE.2012.2227688

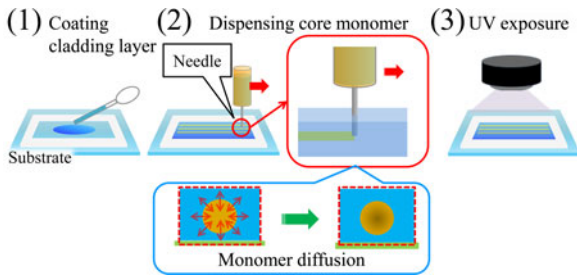


Fig. 1. GI circular-core waveguide fabrication method named “Mosquito method”.

On the other hand, we succeeded in forming almost perfectly circular-shaped cores using a dispenser [16].

Specifically, an innovative method, the “Mosquito method,” is investigated, in which a viscous core monomer is dispensed directly *into* a cladding monomer layer before the cladding monomer is UV cured. Finally, polymer parallel optical waveguides with circular GI-cores are successfully fabricated utilizing the Mosquito method.

The obtained GI circular-core polymer waveguides are characterized and compared to conventional SI square-core polymer waveguides.

In this paper, the fabrication technique for GI-core polymer waveguides is introduced in Section II, and the optical properties of the fabricated waveguides are shown in Section III in which we discuss the feasibility of GI-core polymer waveguide-based O-PCB by comparing the properties with those of SI-core waveguides and even those of a GI MMF. Finally in Section IV, we summarize the results.

II. FABRICATION OF POLYMER PARALLEL OPTICAL WAVEGUIDES

A. Fabrication of Waveguides Using a MicroDispenser

In this paper, a monomer for the core (with high viscosity: $\sim 12\,000$ cPs) is dispensed from a needle, and the waveguide structure is formed by moving the needle in horizontal directions before the UV cure. We use an air-pulse type dispenser system (Musashi Engineering, Inc., ML-808FXcom). In our previous research, we found that it was possible to form a $50\text{-}\mu\text{m}$ core by dispensing the core monomer even from a $190\text{-}\mu\text{m}$ inner-diameter needle, and that a core monomer with a viscosity higher than $22\,500$ cPs was needed for preventing the circular shape from collapsing during the dispensing procedure [16]. However, forming smaller cores requires the adjustment of some other parameters as well as monomer viscosity, and the optimum condition to obtain the desired core diameter has not previously been analyzed. Hence, in this paper, the optimum condition to fabricate circular GI cores with a desired diameter, which would be common to different kinds of waveguide materials (resins), is investigated.

In addition, we introduce the Mosquito method in the following section to form GI-core waveguides very simply, and the obtained waveguides are characterized and compared to the characteristics of conventional SI-type waveguides fabricated by the photolithography method using the same polymer materials.

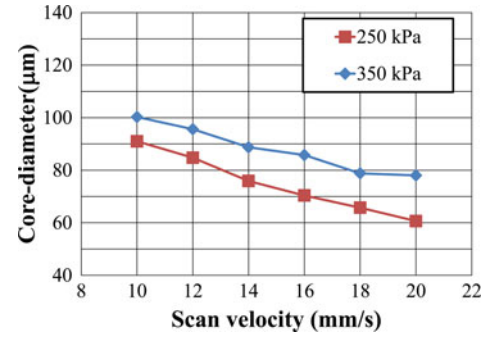


Fig. 2. Core-diameter dependence on dispensing pressure and scan velocity. A needle with a $190\text{-}\mu\text{m}$ inner diameter is used.

B. Mosquito Method

The Mosquito method is illustrated in Fig. 1. First, the viscous monomer for the cladding is coated on a substrate (1). Next, the viscous monomer for core is dispensed *into* the cladding layer by inserting the bottom of the needle, and then the needle is scanned horizontally as shown in the inset (2). Finally, both core and cladding are cured under UV exposure followed by postbaking at $100\text{ }^\circ\text{C}$ (3). The needle scanning for writing the cores is performed using a desktop robot (Musashi Engineering, Inc., SHOT Mini 200DS) customized for the dispenser.

As the waveguide material, UV curable silicone resins (FX-W712 for core: monomer viscosity is $12\,000$ cPs, FX-W713 for cladding: monomer viscosity is $10\,000$ cPs supplied by ADEKA Corporation) are used. Since these monomers are miscible, the core and cladding monomers slightly diffuse into each other to form a concentration distribution before UV exposure, as shown in the inset of Fig. 1. The concentration distribution is fixed by the curing, since the two monomers are three-dimensionally cross-linkable, and form a copolymer. Therefore, the index profiles are quite stable at higher temperatures compared to the dopant-based GI-core polymer waveguides we previously reported [9], [10]. The thermal stability of the waveguides will be evaluated and reported elsewhere.

C. Optimum Dispensing Conditions

For waveguides applied to on-board interconnections, the core size should be less than $100\text{ }\mu\text{m}$, and the current trend is $50\text{ }\mu\text{m}$ and less. Hence, the controllability of the core diameter drawn by the needles is a very important issue. Therefore, the relationship between the dispensed core diameter and dispensing conditions is investigated.

The parameters investigated here are the scanning velocity of the needle, the dispensing pressure, and the needle inner diameter (100 , 130 , 150 , and $190\text{ }\mu\text{m}$).

Figs. 2 and 3 show the experimental results. The plots show the average core diameter. As shown in Figs. 2 and 3, the core diameter can be controlled, and we found that the variation of the core diameter was approximately $\pm 5\%$. In addition, we experimentally confirm that the reproducibility of the core diameter increases with decreasing the inner diameter of the needle, and with increasing the scan velocity.

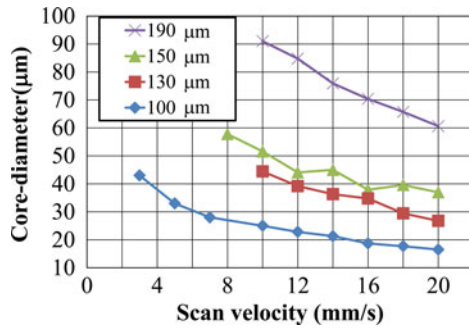


Fig. 3. Core-diameter dependence on needle inner diameter and scan velocity. A uniform dispensing pressure of 250 kPa is adopted.

From Fig. 2, it is found that forming a smaller core requires dispensing under lower pressure and scanning more quickly. From Fig. 3, we can see a needle with a smaller inner diameter forms a smaller core, and a core diameter with a diameter of one-third to one-fifth of the inner diameter of the needle is realized by setting the dispensing conditions appropriately. It should be noted that using needles with less than 150- μm inner diameter (outer diameter 300 μm), a desirable core diameter (smaller than 50 μm) is successfully formed, and moreover, a needle with a 100 μm inner diameter can form a 16.5- μm core diameter, which means fabricating even a single-mode waveguide could be feasible using a slightly thinner needle. We emphasize that the higher needle scanning velocity contributes to forming the core to be close to completely circular. Therefore, from a mass-production point of view, we can say the Mosquito method is a promising fabrication technique.

D. Fabrication of 12-Channel Polymer Parallel Optical Waveguide

From the results in Figs. 2 and 3, we found the appropriate dispensing conditions (e.g. needle diameter, dispensing pressure, and scanning velocity) in order to obtain a desired core diameter. Then, 12-channel parallel waveguides with a 40- μm core diameter and a 250- μm pitch were fabricated successfully (using a needle with a 150- μm inner diameter, 16 mm/s of drawing velocity, and 300 kPa of dispensing pressure). In this method, the gap between the top surface of the substrate and the bottom of the needle is set to be 300 μm in the needle-scanning program for the dispensing robot, while the cladding polymer layer with a sufficient thickness (500 μm) is coated on the substrate. In this case, the distance between the core center and the bottom of the cladding remains constant (about 250 μm). A photograph of 15-cm-long and 5-cm-long waveguides is shown in Fig. 4. In the case of the Mosquito method, the conditions for UV exposure are not as extreme as for the conventional photolithography. Therefore, we can use a small UV-light emitting diode (LED) irradiator, which is also scanned over the waveguide samples using the same desktop robot, and thus, we can fabricate a large-sized waveguide as long as the robot can scan. Furthermore, this Mosquito method could be applied to a mass-production process if we can utilize multiple needles in the roll-to-roll film fabrication process.

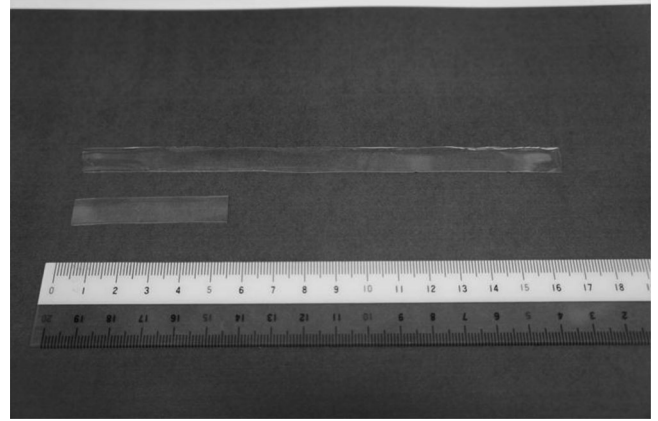


Fig. 4. Photograph of 12-channel GI circular-core polymer optical waveguides fabricated by the Mosquito method.

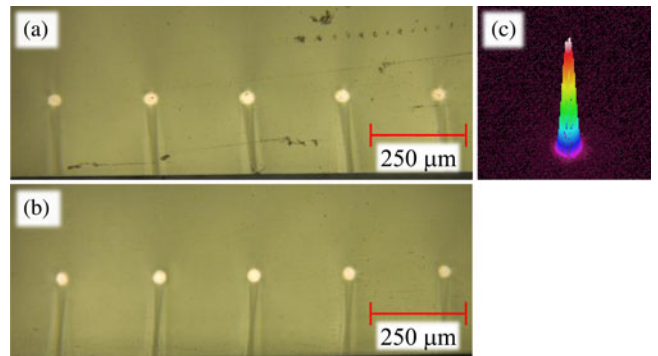


Fig. 5. (a) Cross section of 12-ch-polymer parallel optical waveguide with 40- μm circular core and 250- μm pitch. (b) Cross section of the other edge of the waveguide shown in (a). (c) Near-field pattern from a core of 5-cm-long 12-ch. waveguide.

Fig. 5(a) shows a cross section of the fabricated 12-channel waveguide, while Fig. 5(b) shows the cross section of the other end of the same waveguide shown in Fig. 5(a), where the waveguide length is 5 cm. From the cross section in Fig. 5(a), we analyze the alignment precision of the 12 channels. The pitch length is $255 \pm 3.4 \mu\text{m}$, while the target value is 250 μm . On the other hand, the alignment precision in the vertical direction is evaluated by measuring the distance fluctuation between the core center and the bottom of the waveguide. The standard deviation of the distance is $\pm 2.8 \mu\text{m}$. From the two cross sections shown in Fig. 5 (a) and (b), the high reproducibility of parallel cores in axial directions is also confirmed. Since the positioning precision of the desktop robot (Musashi Engineering, SHOT mini 200DS) is specified as $\pm 10 \mu\text{m}$ [17], the observed reproducibility of the waveguide in this paper is almost within the robot's specification. By using a robot with much higher precision, the deviation of pitch and core alignment are expected to improve. In Section III-E, we will discuss about the effect of core alignment tolerance on coupling losses.

Fig. 5(c) shows the output near-field pattern (NFP) from one core in the 12 channels shown in Fig. 5(a) and (b) after a 5-cm transmission. The NFP is measured using a CCD-based beam profiler (OPHIR Corp., Beam Star_FX50). Here, an LED light

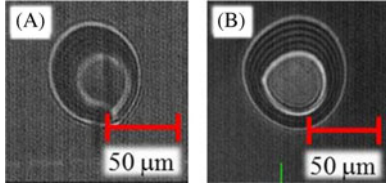


Fig. 6. Interference fringe patterns observed in a core of 12-ch. waveguides A and B fabricated by the Mosquito method.

source at 850 nm is used. In Fig. 5(c), a typical intensity profile from a GI-core waveguide: a strong peak at the core center, gradually decreasing to the periphery (Gaussian-like profile), is observed.

III. CHARACTERIZATION AND DISCUSSION

A. Refractive Index Profile

The refractive index profile of the waveguides fabricated utilizing the Mosquito method is measured using an interference microscope (Mizojiri Optics, TD series). Measured results on two waveguides with different core diameters are shown in Fig. 6 (waveguide A: small core; waveguide B: large core). Concentric interference fringes are observed in the circular core regions, although slight concentricity deviation is observed. The contour-map-like fringe pattern in Fig. 6 indicates that a near-parabolic refractive index profile is formed in the core region. The refractive index profile calculated from the fringe pattern is shown in Fig. 7(a), and Fig. 7(b) shows the 3-D-index profile data on waveguide A. From the data shown in Fig. 7(b) an almost symmetric-index profile is observed, so the concentricity deviation observed in the fringe pattern exhibits little influence on the profile.

It is obvious that a graded-refractive index distribution is formed approximately in the areas of 60 μm and 90 μm diameters in waveguides A and B, respectively, as shown in Fig. 7(a). The core size of waveguide A we estimate from Fig. 6 is slightly larger than the size (40 μm) we measure in the photograph of cross sections shown in Fig. 5. This is probably due to the diffraction effect of the core edge in the image of interference microscope, which is more obvious in smaller cores. Here, the refractive indexes of the core (FX-W712) and cladding (FX-W713) polymers themselves are 1.526 and 1.511, respectively. Therefore, the ideal numerical aperture (NA) of the waveguides composed of these two polymers is calculated to be 0.213. On the other hand, the maximum refractive indexes at the center of waveguide A and B in Fig. 7(a) are 1.519 and 1.526, respectively. Consequently, the calculated NA of waveguide A (with smaller cores) from the index profile data is 0.167. It is predictable that a small core tends to show a lower NA because the core and cladding monomers diffuse sufficiently before the curing process [Fig. 1 (2)]. In order to confirm the accuracy of the index profile measurement, the NAs of the two waveguides are experimentally evaluated using the far-field pattern (FFP) measurement system (Precise Gage, FFP 1005). The results of the two waveguides are summarized in Table I. In the case of waveguide B, the NA calculated from the angular distribution

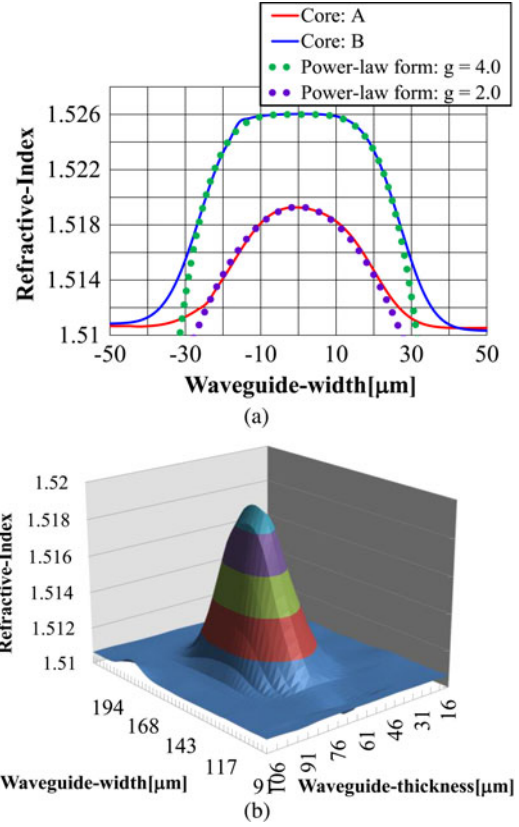


Fig. 7. (a) 2-D refractive index profiles of one core in 12-ch. waveguides A and B fabricated by the Mosquito method. (b) 3-D refractive index profile of a core in 12-ch. waveguide A fabricated by the Mosquito method.

TABLE I
NUMERICAL APERTURES OF WAVEGUIDES A AND B
OBTAINED FROM FFP MEASUREMENT

NA	
Waveguide A	Waveguide B
0.15 - 0.17	0.22 - 0.23

(angular width at 5% intensity) is 0.22 to 0.23, which is almost the same as the ideal value (0.213).

On the other hand, the NA obtained from the FFP results for waveguide A is 0.15 to 0.17, which is almost the same as the NA obtained from the refractive index profile. Thus, the index profiles shown in Fig. 7(a) are accurately measured results. In order to quantitatively analyze the index profile, we approximate the measured index profile by the power-law form described by (1)

$$n(r) = n_1 \left[1 - 2\Delta \left(\frac{r}{a} \right)^g \right]^{\frac{1}{2}} \quad 0 \leq r \leq a \quad (1)$$

$$\Delta = \frac{n_1^2 - n_2^2}{2n_1^2} \quad (2)$$

where r is the distance from the core center to the measuring point, n_1 and n_2 are the refractive indexes at the core center ($r = 0$) and the cladding, respectively, a is the core radius, and g is the index exponent. The g -parameters estimated from the best-fitted curves to the profiles shown in Fig. 7(a) are 2.0 and 4.0 for waveguides A and B, respectively. Just a parabolic index

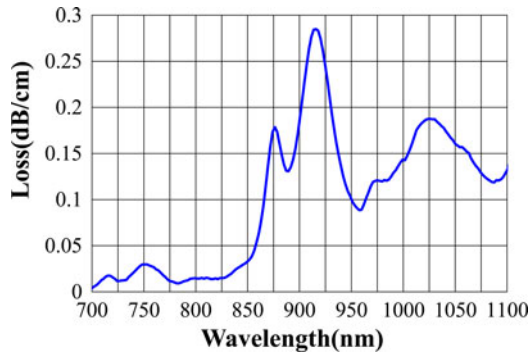


Fig. 8. Propagation loss spectrum of a waveguide fabricated by the Mosquito method.

distribution is formed in the small core, while the profile in the large core is quasi-parabolic. Actually, in the index profile of waveguide B shown in Fig. 7(a), there is a plateau index area with a $25\text{-}\mu\text{m}$ width (from -10 to $15\ \mu\text{m}$ on the horizontal axis). This result clearly shows that the inter diffusion of the core and cladding monomers occurs only in the region around the core-cladding boundary with an approximately $25\text{--}30\text{-}\mu\text{m}$ width. Therefore, when the core diameter is larger than $60\ \mu\text{m}$, we can expect a quasi-parabolic index profile (with a plateau index region) tends to be obtained, and a core diameter of 50 to $60\ \mu\text{m}$ could be the best for obtaining an almost parabolic index profile with ideal NA. On the contrary, too much diffusion of the monomers could occur when the core diameter is less than $50\ \mu\text{m}$. Hence, a lower-than-expected NA value is observed as in the case of waveguide A in Fig. 7(a). For forming a higher NA in such a small core maintaining the ideal parabolic profile, we need to decrease the monomer diffusion; hence, adjusting the monomer viscosity, particularly of the cladding monomer, could be a potential solution.

It is well known that the index exponent values strongly influence the modal dispersion of waveguides. The dispersion and high-speed transmission capability of GI-core waveguides are described elsewhere in detail [18].

B. Propagation Loss

The propagation loss of a waveguide fabricated by the Mosquito method is measured using the cut-back method at a wavelength of $850\ \text{nm}$, which is one of the main wavelengths of VCSELs for MMF links. In this measurement, a halogen-tungsten lamp (white light source) is used, and a $50\text{-}\mu\text{m}\varnothing$ core GI-MMF works as a launching probe to couple the light into a channel of the waveguide. A $100\text{-}\mu\text{m}$ core SI-MMF probe is used to guide the output light from the waveguide to an optical spectrum analyzer. We use a 15-cm -long waveguide.

The obtained propagation loss spectrum is shown in Fig. 8. From the spectrum, the propagation loss of the waveguide at $850\ \text{nm}$ is $0.033\ \text{dB/cm}$, so almost the same or rather lower loss than that ($0.040\ \text{dB/cm}$) of the SI square-core waveguide fabricated by photolithography [6] is obtained. Although the GI-core waveguides are not fabricated in a clean room, such a low loss is achieved. One of the reasons of the low loss is the minimal effect of side-wall roughness in GI-cores.

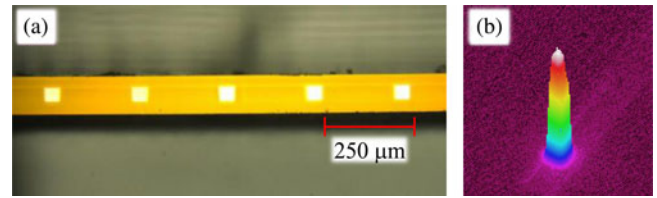


Fig. 9. (a) Cross section of 12 Ch.-polymer parallel optical waveguide with $40 \times 40\ \mu\text{m}$ SI square-cores and $250\text{-}\mu\text{m}$ pitch. (b) Near-Field Pattern through the 5-cm waveguide.

In the spectrum, there is a sharp absorption peak at 875-nm wavelength, and the left shoulder of the peak could influence on the loss at $850\ \text{nm}$. It is already reported that this absorption peak is attributed to the 4th overtone of the carbon-hydrogen stretching vibration involved in aromatic rings [19]. Therefore, reducing the aromatic groups from the core polymer molecules can lead to lower propagation loss at $850\ \text{nm}$.

C. Propagating Mode Field

Output intensity profiles on the edge surface of the GI-core waveguide ($40\text{-}\mu\text{m}$ core in Fig. 5) are measured experimentally and compared with those from the SI square-core (see Fig. 9) waveguide. This waveguide is fabricated utilizing the photolithography method by ADEKA Corp. using the same silicone resins (FX-W712 for core, FX-W713 for cladding). Both the SI core and the GI core are launched via a single-mode fiber (SMF) probe, $25\ \mu\text{m}\varnothing$ or $50\ \mu\text{m}\varnothing$ GI-MMF probe using the same LED light source at $850\ \text{nm}$ as the one we used for Fig. 5(c), and then the output intensities are measured by an NFP camera (Beam Star_FX50). For reducing the effect of speckles on NFPs, we used an incoherent light source.

As shown in Fig. 10, the GI waveguide essentially confines the optical field around the core center, whereas the optical field in the SI core spreads out over its entire core region, except for the case under the SMF-launch. Even when the waveguides are launched via an SMF, the NFP from the GI core is clearly narrower than that from the SI core. When the two waveguides are launched via a 25 and $50\ \mu\text{m}\varnothing$ core GI-MMF probes, the NFPs are almost independent on the kind of launch probe in both waveguides, but slightly narrower NFPs are observed from the GI core than from the SI core. A detailed discussion of this issue will be carried out elsewhere. The strong light confinement confirmed in the GI core could enable highly integrated channel alignment, because it is expected to prevent higher order modes from leaking out from the launched core and to lead to the reduction of inter channel crosstalk. This interchannel crosstalk is discussed in Section III-F in detail.

D. Insertion Loss

In this paper, we assume an O-PCB link comprised of two polymer waveguides (integrated on PCBs) connected by GI-core MMF ribbon(s), as shown in Fig. 11. The lightwave emitted from a VCSEL could be coupled to a waveguide via a 45-degree mirror fabricated on one edge of waveguide. (The mirror is not shown in Fig. 11.) Then the output lightwave from

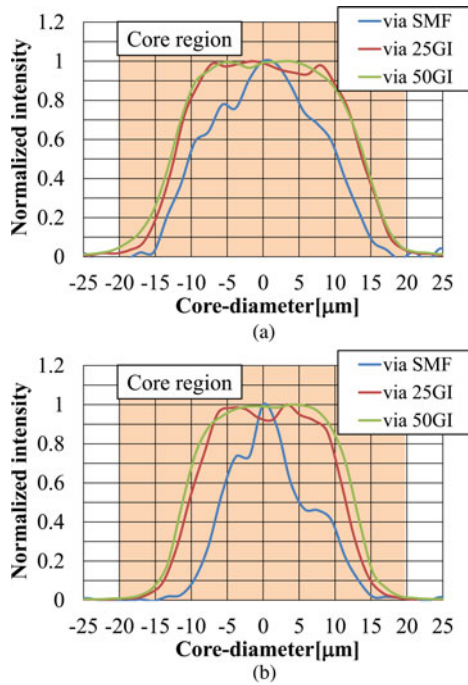


Fig. 10. (a) Output intensity from 40 μm × 40 μm SI square-core. (b) Output intensity profile from 40 μmΦ circular GI-core waveguide.

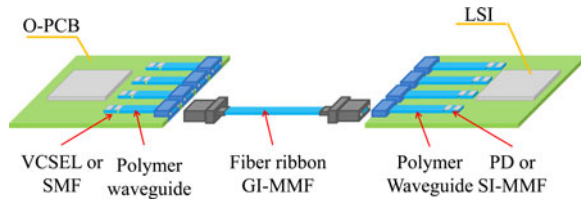


Fig. 11. Design of a polymer waveguide-based optical link for board level optical interconnection.

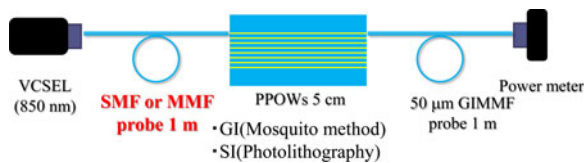


Fig. 12. Experimental setup of the insertion loss.

the waveguide passes through the fiber ribbon and couples to the waveguide on the other board. Finally the light couples into a photo-diode (PD) via a 45° mirror.

For the fabricated waveguide, we measure the insertion loss of a 5-cm-long waveguide at a wavelength of 850 nm. Here, we measure the insertion loss under a realistic condition assuming “real applications” as shown in Fig. 11.

Therefore, the lightwave at 850 nm from a VCSEL is guided by an SMF, a 25- or 50-μm core GI-MMFs, which are utilized for launching a core of the waveguides, and a 50-μm core GI-MMF probe is used to guide the output light from the launched core to an optical power meter, as shown in Fig. 12.

We compare the insertion losses of the SI-core waveguide shown in Fig. 9 and the GI-core waveguide fabricated by the

TABLE II
COMPARISON OF THE AVERAGE INSERTION LOSSES

GI	Launching probe		
	SMF	25 GI	50 GI
Loss[dB]	1.58	1.83	2.52

SI	Launching probe		
	SMF	25 GI	50 GI
Loss[dB]	1.72	2.30	2.68

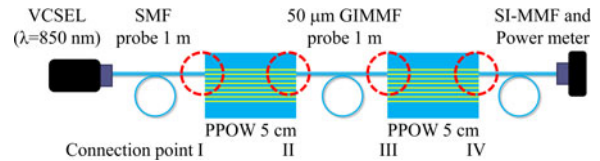


Fig. 13. Measurement system for evaluating the alignment tolerance in the O-PCB link model shown in Fig. 11.

Mosquito method (shown in Fig. 5). The length of both waveguides is set to 5 cm.

Table II shows the average insertion losses of all 12 channels. As the propagation loss of the waveguide at 850 nm is found to be 0.03 to 0.045 dB/cm, the propagation loss of 5-cm waveguide is calculated as 0.15 to 0.23 dB. We did not use a matching oil in this measurement, so approximately 0.2 dB of Fresnel losses could be involved at each connection point between the waveguide and probe. Therefore, 0.55 to 0.63 dB could be the intrinsic insertion loss, and excess losses found in Table II could be attributed to mode-field mismatch at the connection points. Because we use a GI circular-core MMF for the probe, the GI circular-core waveguide we fabricated is advantageous from the mode-field matching point of view, and thus the insertion loss of the GI-core waveguide is lower than that of the SI-core waveguide under any launching conditions. The optical losses due to mode-field mismatching in waveguide and MMF connections are described in [20] in detail.

E. Alignment Tolerance

For applying the GI circular-core polymer waveguides to O-PCBs, the alignment tolerance of waveguides with other optical components (light source, MMFs and detector) is another issue.

In this paper, we use the measurement setup shown in Fig. 13 that is based on the link model shown in Fig. 11, and the alignment tolerance at connection points I, II, III and IV are evaluated. The result obtained at each connection point is shown in Fig. 14. For the waveguides under test, we used the 40 μm diameter GI circular-core waveguide (waveguide A) and 40-μm SI square-core waveguide.

The output light from the SMF does not necessarily realize the output beam from VCSELs. However, we preliminary observed that different output beam qualities were observed among different VCSEL chips and the beam quality was strongly dependent on the bias current. Hence, it is difficult to fix the launching condition at connection point I without a probe fiber. On the other hand, the output NFP from the SMF has almost the same size (~10 μm) as the light emitting area of VCSELs, and the

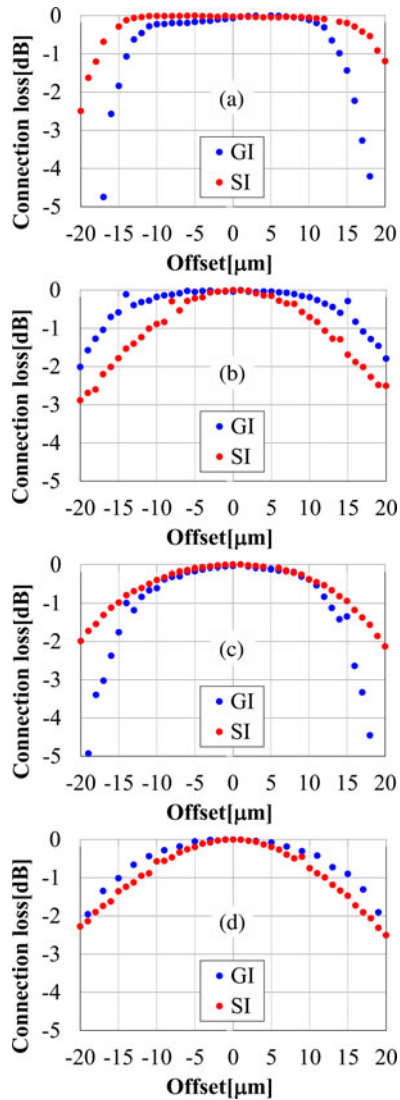


Fig. 14. Alignment tolerance curve of each connection point. (a) I, (b) II, (c) III, and (d) IV.

SMF probe allows the unique launching condition, which is reproducible for all the measurements.

At connection point I, the tolerance curve of the SI-core waveguide is wider than that of the GI core, although the waveguides are launched by an SMF with a small input spot size and low NA. One of the reasons for the small tolerance in the GI waveguide could be the local NA of GI core. If an offset is added to connection point I in the GI-core waveguide link, the local NA of GI-core waveguide could be the same or lower than the NA of SMF, in which case, the coupling loss increases. However, when we evaluated the tolerance curve for the connection between the same SMF and a GI-MMF (substituent for the GI-core waveguide), much wider tolerance is obtained [20] compared to the result in Fig. 14(a). Hence, the local NA of GI-core waveguides is not the main reason. The main reason of the small tolerance could be higher loss of high-order modes. We need to carefully investigate the mode dependent loss, and will report it elsewhere.

The GI core shows much larger tolerance than the SI core at connection point II. This is because there is a small mode-

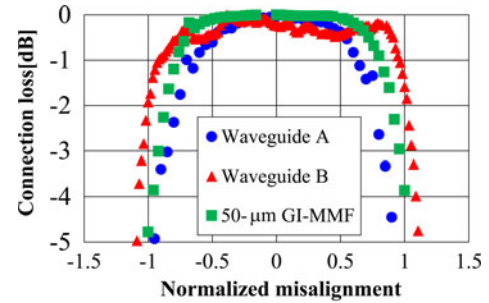


Fig. 15. Comparison of the alignment tolerance curves at connection point III of waveguide A, waveguide B, and 50 $\mu\text{m}\phi$ GI-MMF.

field mismatch in the GI-GI connection, in addition to the small NFP from the GI-core waveguide, as shown in Fig. 10(b). For interboard connections, the use of GI-core MMF is inevitable because of its high modal bandwidth and low loss, and thus, GI circular-core polymer waveguides have an advantage in the connection loss with the MMFs.

When we connect a GI-core waveguide and GI-MMF, in principle, the small spot size and low NA of the SMF-launcher probe at connection point I are well maintained through the GI-core waveguide and GI MMF because of the light confinement effect of the GI core. Hence, we expect that the tolerance curve at connection point III looks very similar to the one at connection point I. Actually, at connection point III, the GI core shows narrower tolerance than the SI core, and the tolerance in GI core is rather narrower than that at connection point I. This narrow tolerance could stem from the low NA (0.16 to 0.17) of the GI-core waveguide (Table I) compared to the NA of MMF (0.22) and from the weaker light confinement in the GI-core waveguide.

Since the NA of waveguide B shown in Figs. 6 and 7 is as high as 0.23, we substitute the GI-core waveguide (waveguide A) for waveguide B, and evaluate the tolerance similarly. Since the core diameter of waveguide B is larger than that of the other waveguides, the tolerance curve is compared by normalizing the horizontal axis with the core radius. The result of the tolerance at connection point III is shown in Fig. 15. Here, the results at connection point III when the GI-core waveguide is replaced by a silica GI-MMF (50 $\mu\text{m}\phi$) are also shown as a comparison. From Fig. 15, the tolerance of waveguide B is much wider than that of waveguide A. Therefore, the narrow alignment tolerance in waveguide A could be improved by increasing the NA, and it would be close to the ideal curve obtained by the GI-MMF. Although the tolerance of waveguide B is rather wider than that of GI-MMF, it could be attributed to the pseudoparabolic profile as shown in Fig. 7(a) or to the larger core size: the local NA of the large GI core decreases moderately against the offset, compared to the small core.

The weak optical confinement of waveguide A is also of concern. We compare the NFP after the 5-cm propagation through waveguide A with the NFPs after 1-m-long 35- and 50- $\mu\text{m}\phi$ GI-MMFs. Fig. 16 shows the results. The measurement condition is the same as that shown in Fig. 10, and the SMF probe is used for launching. It is obvious that the NFP from the GI-MMF is much narrower than that of the GI-core waveguide

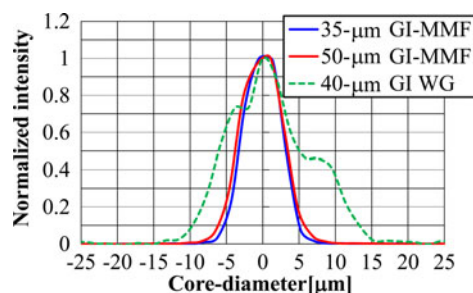


Fig. 16. Comparison of output NFPs from GI-core waveguide (waveguide A), $35\ \mu\text{m}$ diameter GI-MMF, and $50\ \mu\text{m}$ diameter GI-MMF when they are launched via an SMF probe.

(waveguide A). Therefore, the output NFP from waveguide A at connection point II is already much wider than that from the SMF probe, and the wider profile is transferred by the GI MMF from connection point II to connection point III. And then, the narrow tolerance in GI waveguide at connection point III is observed as in Fig. 14(c), as the combined effect of the low NA in waveguide A.

Strong mode conversion from low-order modes to high-order modes in the GI-core polymer waveguide is one of the reasons why the output NFP is wide [12], [21], as shown in Fig. 16. Therefore, by reducing the excess scattering loss in GI-core polymer waveguides for lowering the mode conversion, low connection loss and wide alignment tolerance similar to the GI-MMF case could be realized.

Meanwhile, in terms of the connection between light sources and waveguides, recent trends are in using lens systems for high coupling efficiency. In particular, some reports show the possibility even using two lenses for the light coupling from a VCSEL to a waveguide via an optical via hole [22].

If the light coupling with lens systems is utilized, it would require optimizing the launching condition for GI-core waveguides, as discussed in the case of the launch condition for GI-MMFs for Ethernet standardization [23].

For optimizing the launch condition, the loss at connection point II is evaluated, when a lensed GI-MMF (Moritex corp., CT980G5/BC10FS-N) is adopted instead of the SMF probe for launching the GI-core waveguide at connection point I. A launch NA of 0.28 could be achieved using the lensed GI-MMF, while the minimum spot size could be approximately $2.1\ \mu\text{m}$ at the focal point. The misalignment tolerance of the GI-core waveguide (Waveguide A) at connection point II is $34\ \mu\text{m}$ for 1-dB loss tolerance under the lensed GI-MMF launch condition, while $36\ \mu\text{m}$ under the SMF launch condition. The reason of the misalignment tolerance degradation under the lensed GI-MMF launch is very small is because the NA of the waveguide A is as low as 0.17. The influence of launching condition would be more obvious when we use a GI-core waveguide with higher NA. Hence, the launch condition optimization should be very important for the GI-core waveguides in order to achieve a good connectivity with the other optical components.

F. Interchannel Crosstalk

As mentioned earlier, GI cores have the potential to tightly confine the optical field near the core center, so we have been

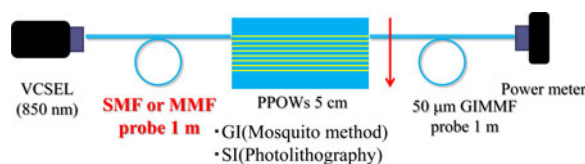


Fig. 17. Experimental setup for measuring crosstalk.

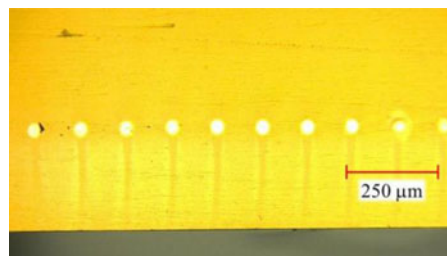


Fig. 18. Cross section of a $125\text{-}\mu\text{m}$ pitch waveguide.

promoting the capability of high-density channel alignment by the GI core, in particular, its very narrow pitch [9]–[13]. Actually, we simulated how we can decrease the intercore pitch while maintaining an interchannel crosstalk lower than $-20\ \text{dB}$ for both GI and SI cores. Then, we showed that the minimum pitch of GI-core waveguides could be smaller than that of SI-core waveguides [24]. On the other hand, it has been difficult to fairly compare the interchannel crosstalk of SI- and GI-core waveguides experimentally so far, because the SI- and GI-core waveguides fabricated using the same polymer materials have not been available. In our previous report [10], we fabricated both SI- and GI-core waveguides satisfying the conditions for a fair comparison of the crosstalk using the soft-lithography method, and could show lower crosstalk in the GI-core waveguide than in the SI counterpart. However, the waveguides obtained had a propagation loss as high as $0.1\ \text{dB/cm}$ at $850\ \text{nm}$. Hence, the excess scattering loss of the waveguides enhanced mode conversion and lead to a high crosstalk ($-20\ \text{dB}$), even in the GI-core waveguide despite sufficiently wide pitch ($250\ \mu\text{m}$).

Therefore, in this paper, we experimentally compare the crosstalk of the SI- and GI-core waveguides composed of the same polymer materials with sufficiently low propagation loss, for the first time to the best of our knowledge. The interchannel crosstalk is measured using the setup schematically shown in Fig. 17. First, we measure the output power from the launched core after a 5 cm waveguide transmission, where the center of the core at one edge in 12 cores is launched via an SMF or $25\text{-}\mu\text{m}$ diameter GI-MMF probe. The output power from the launched core is detected by an optical power meter via a $50\text{-}\mu\text{m}$ diameter GIMMF. Next, as shown in Fig. 17, the detection probe (GI-MMF) is scanned horizontally with a step of $1\ \mu\text{m}$ for detecting the output power from other 11 cores.

In addition, since the waveguide with a pitch narrower than $250\ \mu\text{m}$ would be required for high-density wiring, a 12-channel GI circular-core waveguide with a $40\text{-}\mu\text{m}$ core diameter and a $125\text{-}\mu\text{m}$ pitch is fabricated using the Mosquito method. A cross section of the obtained waveguide is shown in Fig. 18.

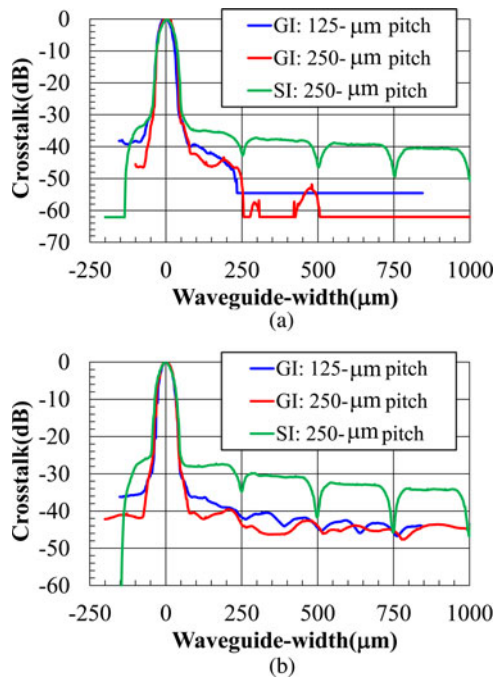


Fig. 19. (a) Interchannel crosstalk measurement results of the GI- and SI-core waveguide launched by an SMF probe. (b) Interchannel crosstalk measurement results of the GI- and SI-core waveguide launched by a $25\ \mu\text{m}\varnothing$ GI-MMF probe.

Even in the case of $125\text{-}\mu\text{m}$ pitch, GI circular-cores are well aligned with a good reproducibility in pitch. The reproducibility of the pitch is slightly higher than in the $250\text{-}\mu\text{m}$ pitch waveguide. One of the concerns in reducing the pitch is an increase in interchannel crosstalk. Therefore, we compare the interchannel crosstalk in the narrow-pitch waveguide to that in the $250\text{-}\mu\text{m}$ pitch waveguide.

Fig. 19(a) and (b) compare the results of GI- and SI-core waveguides. The GI-core waveguides exhibit lower crosstalk than the SI-core. Even if the waveguides are launched via an SMF probe [in Fig. 19(a)], the SI-core waveguide shows higher crosstalk than the GI-core waveguide, although the measured value of $-42\ \text{dB}$ is sufficiently low.

It is found from Fig. 19 that the output power from the *cladding* is quite high in the case of SI-core waveguide regardless of the launching conditions. On the other hand, when the detection probe is just aligned to the neighboring cores, the output power abruptly decreases, and dips are observed in the curves. The high output power from the cladding of SI-core could be caused by the light leaking out from the launched core, probably due to rough core-cladding surface.

It is interesting that the SI-core waveguide used in this measurement also exhibited sufficiently low propagation loss ($0.045\ \text{dB/cm}$). However, even though only a slight amount of light leaked out to the cladding, it can also be confined “in the cladding” by the internal reflection at the boundary between the cladding and the outside medium (mainly air). Then, the *cladding-mode* is influencing the interchannel crosstalk. The crosstalk is also caused by the mode conversion from the cladding modes to propagating modes in the neighbor cores. Hence, if the outside of SI-core waveguide is coated with a high

TABLE III
COMPARISON OF CROSSTALK VALUES IN GI-CORE AND SI-CORE WAVEGUIDES UNDER DIFFERENT LAUNCH CONDITIONS IN DECIBEL

Waveguide	Probe	Ch. 2	Ch. 3	Ch. 4
Waveguide A	SMF	-52.1	-57.4	<-62.0
GI($125\ \mu\text{m}$)		-41.1	-54.6	-54.6
SI		-42.2	-46.5	-49.0
Waveguide A	$25\ \mu\text{m}\varnothing$ GI-MMF	-43.6	-44.0	-45.2
GI($125\ \mu\text{m}$)		-36.4	-41.6	-42.9
SI		-34.8	-41.7	-45.8
Waveguide A	$50\ \mu\text{m}\varnothing$ GI-MMF	-29.3	-28.0	-30.3
Waveguide B		-36.5	-36.0	-37.7
SI		-30.3	-33.7	-37.0

index or absorptive medium for lowering the power of cladding mode, the crosstalk in the SI-core waveguides may decrease.

In Table III, the observed crosstalk values are summarized. Here, the crosstalk in GI-core waveguides (Waveguide A, B, and SI-core waveguide) when $50\text{-}\mu\text{m}\varnothing$ GI-MMF is used for the launch probe is also shown in order to discuss the influence of launch condition. It is clear that the crosstalk values are quite low, compared to those previously observed in the waveguides fabricated by the soft-lithography method (approximately $-20\ \text{dB}$) [10]. As we mentioned earlier, the propagation losses of both waveguides (SI and GI cores) used in this paper are very low (0.033 to $0.045\ \text{dB/cm}$), the mode conversion from the propagating modes to the cladding modes and vice versa is also quite small compared to the waveguide fabricated using the soft lithography. That is why the crosstalk is reduced to such a small value. However, under the same pitch size condition ($250\ \mu\text{m}$), the GI-core waveguide exhibits approximately $10\ \text{dB}$ lower crosstalk than the SI-core counterpart when they are launched using the SMF and $25\text{-}\mu\text{m}\varnothing$ GI-MMF probes. Contrastingly, in the case of half-pitch GI-core waveguides, about $10\ \text{dB}$ of crosstalk increase is observed in the adjacent core (Ch. 2) under the same launch conditions. However, the crosstalk in the $125\text{-}\mu\text{m}$ pitch GI-core waveguide is low enough to maintain almost the same level as that in the $250\text{-}\mu\text{m}$ pitch SI-core waveguide. Thus, the light confinement in the cores is very important for maintaining low crosstalk, and we experimentally confirm the capability of high-density alignment in polymer waveguides by applying GI cores to them.

Meanwhile, when Waveguides A and B are launched using a $50\text{-}\mu\text{m}\varnothing$ GI-MMF probe, the crosstalk of Waveguide A is almost the same as that of the SI-core waveguide. With increasing the core diameter of the probe, the uncoupled light to the core of waveguide also increases, resulting in high intensity of the cladding modes. The cladding modes could recouple to the propagating modes in the adjacent cores to increase the crosstalk.

In particular, the low NA of Waveguide A could contribute to the additional crosstalk increase. Therefore, the crosstalk of Waveguide B with high NA (0.23) is maintained low compared to those of Waveguide A and SI-core waveguide, as shown in Table III. From these results, GI-core waveguides with the same or higher NA than the launching probe should be used.

IV. CONCLUSION

We successfully fabricated 12-channel polymer parallel optical waveguides with GI circular cores by the Mosquito method.

We found the dispensing condition in order to form the cores of 50 $\mu\text{m}\phi$ and less while completely maintaining a circular-core shape; the reproducibility of cores was also confirmed. The propagation loss of the fabricated waveguide is very low (0.033 dB/cm at 850 nm), which is comparable or lower than the SI square-core waveguide composed of the same silicone polymers. We also compared other optical properties such as insertion loss, misalignment tolerance, interchannel crosstalk of the GI-core waveguides with those of the SI-core counterparts. This is the first comparison, to the best of our knowledge, between SI square-core and GI circular-core multimode polymer waveguides composed of the same material with sufficiently low optical loss. The GI-core waveguide exhibits lower insertion loss and lower crosstalk (approximately 10 dB) than the SI-core waveguide. In addition, even if the pitch of the GI-core waveguide is reduced to the half of 250 μm , the crosstalk of GI-core waveguide is almost the same or lower than that in the 250- μm pitch SI-core waveguide. These remarkable properties of GI-core waveguides are attributed to the tight optical field confinement at the core center in the GI core. Thus, the Mosquito method introduced in this paper is a promising method to simply fabricate polymer parallel optical waveguide with GI circular-core for O-PCB applications.

ACKNOWLEDGMENT

The authors would like to thank Dr. Y. Ishikawa of ADEKA Corporation for the silicone polymer material supply and for his continuous technical support to this research.

REFERENCES

- [1] A. Benner, M. Ignatowski, J. A. Kash, D. M. Kuchta, and M. B. Ritter, "Exploitation of optical interconnects in future server architectures," *IBM J. Res. Dev.*, vol. 49, no. 4 and 5, pp. 755–775, 2005.
- [2] D. Glice, H. Brandt, C. Wright, P. McCarthy, A. Emerich, T. Schimke, C. Archer, J. Carey, P. Sanders, J. A. Fritzjunker, S. Lewis, and P. Germann, "Breaking the petaflops barrier," *IBM J. Res. Dev.*, vol. 53, no. 5, pp. 1:1–1:16, 2009.
- [3] F. E. Doany, C. L. Schow, B. G. Lee, R. A. Budd, C. W. Baks, C. K. Tsang, J. U. Knickerbocker, R. Dangel, B. Chan, H. Lin, C. Carver, J. Huang, J. Berry, D. Bajkowski, F. Libsch, and J. A. Kash, "Terabit/s-class optical PCB links incorporating 360-Gb/s bidirectional 850 nm parallel optical transceivers," *J. Lightw. Technol.*, vol. 30, no. 4, pp. 560–571, Feb. 2012.
- [4] Y. Matsuoka, D. Kawamura, K. Adachi, Y. Lee, S. Hamamura, T. Takai, T. Shibata, H. Masuda, N. Chujo, and T. Sugawara, "20-Gb/s/ch high-speed low-power 1-Tb/s multilayer optical printed circuit board with lens-integrated optical devices and CMOS IC," *IEEE Photon. Technol. Lett.*, vol. 23, no. 18, pp. 1352–1354, Sep. 2011.
- [5] S. Uhlig, L. Fröhlich, M. Chen, N. Arndt-Staufenbiel, G. Lang, H. Schröder, R. Houbertz, M. Popall, and M. Robertsson, "Polymer optical interconnects—A scalable large-area panel processing approach," *IEEE Trans. Adv. Packag.*, vol. 29, no. 1, pp. 158–170, Feb. 2006.
- [6] K. Hara, Y. Ishikawa, and Y. Shoji, "Preparation and properties of novel silicone-based flexible optical waveguide," *Proc. SPIE*, vol. 6376, pp. 63760K-1–63760K-10, Oct. 2006.
- [7] T. Mori, K. Takahama, M. Fujiwara, K. Watanabe, H. Owari, Y. Shirato, S. Terada, M. Sakamoto, and K. Choki, "Optical and electrical hybrid flexible printed circuit boards with unique photo-defined polymer waveguide layers," *Proc. SPIE*, vol. 7607, pp. 76070S-1–76070S-11, 2010.
- [8] N. Bamiedakis, J. Beals, IV, R. V. Penty, I. H. White, J. V. DeGroot, jr., and T. V. Clapp, "Cost-effective multimode polymer waveguides for high-speed on-board optical interconnects," *IEEE J. Quantum. Electron.*, vol. 45, no. 4, pp. 415–424, Apr. 2009.
- [9] Y. Takeyoshi and T. Ishigure, "High-density 2×4 channel polymer optical waveguide with graded-index circular cores," *J. Lightw. Technol.*, vol. 27, no. 14, p. 2852–2861, Jul. 2009.

- [10] T. Ishigure and Y. Nitta, "Polymer optical waveguide with multiple graded-index cores for on-board interconnects fabricated using soft-lithography," *Opt. Express*, vol. 18, no. 13, pp. 14191–14201, Jun. 2010.
- [11] T. Kosugi and T. Ishigure, "Polymer parallel optical waveguide with graded-index rectangular cores and its dispersion analysis," *Opt. Express*, vol. 17, no. 18, pp. 15959–15968, 2009.
- [12] H-H. Hsu and T. Ishigure, "High-density alignment of graded-index core polymer optical waveguide and its crosstalk analysis with ray tracing method," *Opt. Express*, vol. 18, no. 13, pp. 13368–13378, Aug. 2010.
- [13] H-H. Hsu, Y. Hirobe, and T. Ishigure, "Fabrication and inter-channel crosstalk analysis of polymer optical waveguides with W-shaped index profile for high-density optical interconnections," *Opt. Express*, vol. 19, no. 15, pp. 14018–14030, Jul. 2011.
- [14] Y. Leng, V. Yun, L. Lucas, W. N. Herman, and J. Goldhar, "Dispensed polymer waveguides and laser-fabricated couplers for optical interconnects on printed circuit boards," *Appl. Opt.*, vol. 46, no. 4, pp. 602–610, Feb. 2007.
- [15] J. Chappel, D. A. Hutt, and P. P. Conway, "Variation in the line stability of an inkjet printed optical waveguide-applicable material," in *Proc. 2nd Electron. System integr. Technol. Conf.*, 2008, pp. 1267–1272.
- [16] S. Morikawa and T. Ishigure, "Fabrication of GI-core polymer optical waveguide using a dispenser and its application to optical printed circuit boards," in *Proc. Annu. IEEE Photon. Soc. Meeting*, 2010, pp. 1–4.
- [17] Musashi Engineering, Inc. Ultimately compact desk-top robot, SHOTmini 100 s. (2012). [Online]. Available: http://www.musashi-engineering.co.jp/english/products/179_3-4-1-4.html
- [18] S. Yakabe, K. Shitanda, T. Ishigure, and S. Nakagawa, "High-bandwidth density and low-power optical PCB using GI-core polymer waveguide," *IEEE J. Sel. Topics. Quantum Electron.*, to be published.
- [19] A. Tanaka, H. Sawada, and N. Wakatsuki, "New plastic optical fiber using polycarbonate core," *Fujitsu Sci. Tech. J.*, vol. 23, no. 3, pp. 166–176, Sep. 1987.
- [20] S. Yakabe, T. Ishigure, and S. Nakamura, "Link power budget advantage in GI-core polymer optical waveguide link for optical printed circuit boards," *Proc. SPIE*, vol. 8267, pp. 8267 J-1–8267 J-5, 2012.
- [21] T. Ishigure, K. Ohdoko, Y. Ishiyama, and Y. Koike, "Mode-coupling control and new index profile of GI POF for restricted-launch condition in very-short-reach networks," *J. Lightw. Technol.*, vol. 23, no. 12, pp. 4155–4168, Dec. 2005.
- [22] F. E. Doany, C. L. Schow, B. G. Lee, R. Budd, C. Baks, R. Dangel, R. John, F. Libsch, J. A. Kash, B. Chan, H. Lin, C. Carver, J. Huang, J. Berry, and D. Bajkowski, "Terabit/sec-class board-level optical interconnects through polymer waveguides using 24-channel bidirectional transceiver modules," in *Proc. 62nd Electron. Compon. Technol. Conf.*, 2012, pp. 790–797.
- [23] P. Pepeljugoski, M. J. Hackert, J. S. Abbott, S. E. Swanson, S. E. Golowich, A. J. Ritger, P. Kolesar, Y. C. Chen, and P. Pleunis, "Development of system specification for laser-optimized 50- μm multimode fiber for multigigabit short-wavelength LANs," *J. Lightw. Technol.*, vol. 21, no. 5, pp. 1256–1275, May 2003.
- [24] T. Ishigure, R. Ishiguro, H. Uno, and H-H. Hsu, "Maximum channel density in multimode optical waveguides for parallel interconnections," in *Proc. 61st Electron. Compon. Technol. Conf.*, 2011, pp. 1847–1851.



Kazutomu Soma was born in Shizuoka, Japan on May 28, 1988. He received the B.S. degree in applied physics and physico informatics from Keio University, Yokohama, Japan, in 2011, where he is currently working toward the M.S. degree in integrated design functions.

In April 2013, he will join SoftBank. His current research interests include fabrication of polymer parallel optical waveguide with GI circular-core by using a micro dispenser and its optical properties toward high-speed and high-density optical interconnection.



Takaaki Ishigure (M'00) was born in Gifu, Japan, on July 30, 1968. He received the B.S. degree in applied chemistry, and the M.S. and Ph.D. degrees in material science from Keio University, Yokohama, Japan, in 1991, 1993, and 1996, respectively.

He is currently an Associate Professor at Keio University. In 2005, he was with the Department of Electrical Engineering, Columbia University, New York, as a Visiting Research Scientist. His current research interest includes on-board optical interconnections realized with multimode polymer optical waveguides.